Critical Interplay between Parasite Differentiation, Host Immunity, and Antigenic Variation in Trypanosome Infections

E. Gjini,[1,2,*] D. T. Haydon,[2,3,4] J. D. Barry,[4,5] and C. A. Cobbold[1,2]

1. Department of Mathematics, University of Glasgow, University Gardens, Glasgow G12 8QW, United Kingdom; 2. The Boyd Orr Centre for Population and Ecosystem Health, University of Glasgow, United Kingdom; 3. Faculty of Biomedical and Life Sciences, Ecology and Evolutionary Biology, University of Glasgow, Glasgow G12 8QQ, United Kingdom; 4. Wellcome Trust Centre for Molecular Parasitology, University of Glasgow, United Kingdom; 5. Glasgow Biomedical Research Centre, 120 University Place, Glasgow G12 8TA, United Kingdom

Submitted May 19, 2010; Accepted June 23, 2010; Electronically published August 17, 2010

ABSTRACT: Increasing availability of pathogen genomic data offers new opportunities to understand the fundamental mechanisms of immune evasion and pathogen population dynamics during chronic infection. Motivated by the growing knowledge on the antigenic variation system of the sleeping sickness parasite, the African trypanosome, we introduce a mechanistic framework for modeling within-host infection dynamics. Our analysis focuses first on a single parasitemia peak and then on the dynamics of multiple peaks that rely on stochastic switching between groups of parasite variants. A major feature of trypanosome infections is the interaction between variant-specific host immunity and density-dependent parasite differentiation to transmission life stages. In this study, we investigate how the interplay between these two types of control depends on the modular structure of the parasite antigenic archive. Our model shows that the degree of synchronization in stochastic variant emergence determines the relative dominance of general over specific control within a single peak. A requirement for multiple-peak dynamics is a critical switch rate between blocks of antigenic variants, which implies constraints on variant surface glycoprotein (VSG) archive genetic diversification. Our study illustrates the importance of quantifying the links between parasite genetics and within-host dynamics and provides insights into the evolution of trypanosomes.

Keywords: African trypanosome, within-host dynamics, antigenic variation, VSG archive structure, specific and general control, carrying capacity.

Introduction

Pathogens interact with their hosts in complex ways, using subtle strategies for immune evasion and for establishing chronic infection (Frank 2002; Schmid-Hempel 2008). One of the most sophisticated parasite survival strategies is antigenic variation, where individuals within the proliferating parasite population switch to expression of an alternative form of a major antigen. This allows the parasite to avoid impending antibody responses and characteristically yields an oscillating parasite load over long periods. The most intensively studied parasite antigenic variation system is that of the African trypanosome (Barry and McCulloch 2001). *Trypanosoma brucei* is a protozoan, transmitted by the tsetse fly, that can infect a wide range of host species, including humans, livestock, and wild mammals, generally causing chronic diseases such as human sleeping sickness. Recent advances in our understanding of the trypanosome genome and its genetic archive encoding antigenically variable coat proteins motivates the need for a common framework, where parasite genetic processes and within-host dynamics can be integrated.

Trypanosomes have a coat composed of variant surface glycoprotein (VSG) that undergoes antigenic variation, through the sequential replacement of different VSG genes in expression sites (Berriman et al. 2005). Different VSG genes are selected through a switching process from an archive of ~2,000 silent VSG genes encoding different forms of this protein. This seemingly simple genetic basis for variation is compounded at the within-host population level, however, by a number of parasite processes, including growth, death, and differentiation, and host processes, most notably acquired immune responses against the antigens that are subject to antigenic variation. Typical of antigenic variation, trypanosome infections show hierarchical variant expression in which some variants appear early in infections and others appear progressively later (Gray 1965; Capbern et al. 1977; Kosinski 1980; Barry 1986; Morrison et al. 2005). This hierarchical expression is mediated by the magnitudes of switch rates between different antigenic variants, which in turn result from ge-

* Corresponding author; e-mail: egjini@maths.gla.ac.uk.

Am. Nat. 2010. Vol. 176, pp. 000–000.
DOI: 10.1086/656276

netic properties of the VSG archive, such as the locus types in the genome (Barry 1997; Turner 1999; Morrison et al. 2005; Marcello and Barry 2007*a*). Furthermore, most archive VSG genes are pseudogenes that can be expressed only after recombining with other members of the archive to produce an intact, mosaic gene, a set of events that occur with low probability. Within each locus type, there appear to be finer degrees of ordering, and the prevailing view is that switch rates range widely, in particular over discontinuous orders of magnitude (Frank 1999; Lythgoe et al. 2007).

A considerable amount is known about parasite and host factors compounding antigenic variation in trypanosomes. In the mammalian host, the dividing slender form differentiates to the nondividing stumpy stage, which is the only life stage that can infect the tsetse (Dean et al. 2009). This process is density dependent, and its major characteristics have been quantified (Reuner et al. 1997). Besides serving as a proxy for transmission, the stumpy stage, by virtue of its quiescence and fixed life span, contributes to self-regulation of growth of the within-host parasite population. The population reaches a maximum carrying capacity, which has been measured in immunosuppressed hosts and which has been shown to equal the maximum height of growth peaks in normal infections (Balber 1972; Luckins 1972; Hajduk and Vickerman 1981). There is also symmetry in growth across different variants. Thus, there is maximally only 10% variance in the growth rates of trypanosome clones isolated from the same infection, and any differences do not correlate with the VSG expressed (Seed 1978). In addition, the kinetics of induction of immunity (Gray 1965) and variant clearance (Hajduk and Vickerman 1981) are common between variants. The general picture, at least for variants that appear early in infection, is that variant-specific responses arise rapidly and persist for prolonged periods (Gray 1965; Morrison et al. 2005).

The structure and organization of the VSG archive have been elucidated in increasing detail over the past years. It has emerged that VSG genes are organized into subfamilies of closely related genes, displaying high levels of genetic identity. In the chronic phase of infection, when mosaic variants appear, there is evidence that genetic identity between subfamilies plays an important role in determining between-variant switch rates (Thon et al. 1990; Marcello and Barry 2007*a*). These findings suggest a pattern of higher switch rates for genes within subfamilies and lower switch rates for genes between subfamilies (Thon et al. 1990; Marcello and Barry 2007*a*).

In this study, we propose a mathematical model with which we can understand mechanistically what drives trypanosome antigenic variation over the course of an infection and how chronicity is maintained. We focus on the interplay between the structure of the antigenic archive, mirrored in the switch rates, and within-host processes, such as parasite differentiation and the specific immune response. A better understanding of this interplay could be instrumental in the design of control strategies and further experimental research. We study different aspects of chronic infection dynamics and a wide range of possible infection scenarios, such as oscillating parasite loads and the antigenic composition of each peak. Finally, we consider simple model extensions that include immunosuppression and cross-reactive immunity.

Model

Variant Dynamics

Our model is formulated to capture the primary features of within-host trypanosome dynamics, and it advances the model proposed by Lythgoe et al. (2007). We distinguish two within-host forms of the parasite: slender and stumpy. We denote the parasite number in the ith variant subpopulation as $i = 1, \ldots, N$, with v_i and m_i for slender and stumpy cells, respectively, and a_i for the variant-specific antibody response. The size of the parasite antigen gene archive is shown as N.

The dynamics for each variant and antibody response (see fig. 1*A*) are given by

$$\frac{dv_i}{dt} = rv_i\left(1 - \frac{V + M}{K}\right) - da_iv_i, \tag{1}$$

$$\frac{dm_i}{dt} = rv_i\frac{V + M}{K} - \delta a_im_i - \delta_M m_i, \tag{2}$$

$$\frac{da_i}{dt} = c\left[\frac{v_i(t - \tau) + m_i(t - \tau)}{C}\right]^x(1 - a_i), \tag{3}$$

where $V = \sum_i v_i$ and $M = \sum_i m_i$ represent the total number of slender and stumpy parasites. Each slender cell divides with an intrinsic per capita division rate, r, which is a constant throughout the infection and does not decay exponentially, as in the Lythgoe model (Lythgoe et al. 2007). An exponentially decaying r as a function of time blocks parasite replication independently of the immune response after some time, and this assumption is not realistic. A key feature of parasite dynamics is the density-dependent differentiation of each slender cell to the stumpy form, where K is the total within-host carrying capacity. Our choice of the differentiation rate $rv_i(V + M)/K$ differs from the exponential function used by Lythgoe et al. (2007). While other more complicated functions of density dependence are possible, given the lack of firm biological basis for one form over another, the simpler

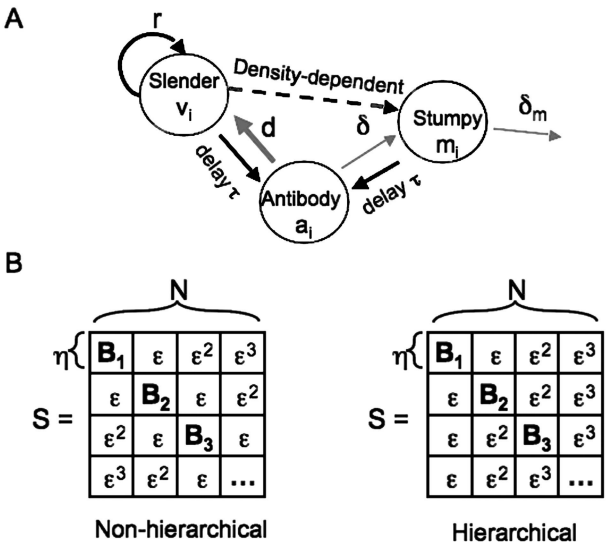

Figure 1: Model ingredients. *A*, Diagram illustrating the deterministic infection dynamics for an arbitrary variant. *B*, Schematic representation of the switch matrix **S**. Antigenic variants are organized in blocks of η variants each, where switching happens fast. Between-block switch rates are of lower-order magnitudes. The nonhierarchical mode assumes only the distance between blocks determines their switch rate (power law distribution). The hierarchical mode assumes each block has an intrinsic activation rate governing their order of appearance. In the simulations we use mainly the nonhierarchical switch matrix, but the results apply to both types. Ultimately, the real trypanosome archive may contain a combination of hierarchical and nonhierarchical variant organization.

logistic form we adopt has the advantage of mimicking infection dynamics in the absence of immune control, both in terms of an oscillatory approach to a clear carrying capacity with the right slender-to-stumpy ratio and the advantage of being more amenable to analytic treatment. Each stumpy cell has a natural mortality δ_M, (McLintock et al. 1993; Tyler et al. 2001). This parameter was absent in the model of Lythgoe et al. (2007), but we find its inclusion is very important for the parasite population dynamics. There is not a similar death rate of the slender cells in the model because eventually the phenomenon can be implicitly captured by a corresponding reduction in the parameters r and K.

For the kinetics of the immune response we follow the same approach as Lythgoe et al. (2007). The ith variant is removed by a specific antibody response a_i at a rate d for slender cells and δ for stumpy cells. Given the evidence that slender cells are killed more rapidly by the immune response, we assume $d > \delta$ (McLintock et al. 1993). Variant-specific antibody responses grow as a result of antigen stimulation, up to a maximum of 1, starting from 0. The maximum rate at which the immune response can increase against any variant i is given by c, meaning that all variants are equally immunogenic, as supported by observations in vivo (Gray 1965). The time that it takes for a variant to stimulate the specific immune response in the host (Tyler et al. 2001), gives the delay τ in equation (3). The sensitivity of the specific immune response to low antigen stimulation is denoted by x, which slows down the saturation of a_i when the ith parasite variant subpopulaton is below the threshold C and accelerates it when the variant population exceeds C. This baseline formulation assumes that high and prolonged parasitemias or antigenic diversity do not significantly impair the anti-VSG immune response, as observed in infections (Gray 1965; Capbern et al. 1977; Robinson et al. 1999; Morrison et al. 2005). Last, under the generality that specific memory B cells develop in parallel with the primary immune response in trypanosome infections, we factor that specific immune responses persist, as observed empirically (Robinson et al. 1999; Morrison et al. 2005). This irreversibility of the immune response prohibits second or further outbreaks by the same antigen variant in the same infection, making chronicity an exclusive consequence of parasite antigenic variation. Model parameters are summarized in table 1.

Variant Emergence

When a new parasite variant arises during infection, its number is very small, and it may be prone to extinction. For this reason, the emergence of new variants is more appropriately modeled as a stochastic process. Differently from Lythgoe et al. (2007), we include a stochastic component in the model in terms of random first-arrival times for each variant t_i. Under this new framework, the slender variant dynamics (eq. [1]) becomes

$$\frac{dv_i}{dt} = \left[rv_i\left(1 - \frac{V + M}{K}\right) - da_iv_i\right]H(t - t_i) + D(t - t_i), \quad (4)$$

where $H(t - t_i)$ and $D(t - t_i)$ are the Heaviside and Dirac delta functions, respectively. Term $H(t - t_i)$ is 0 for $t < t_i$ and 1 for $t \geq t_i$, whereas $D(t - t_i)$ is 0 everywhere except at $t = t_i$, where it takes the value of 1. The stochastic arrival times t_i are determined through a Markov process, similar to the approach of Kepler and Perelson (1995). First, we denote by s_{ij} the rate of antigenic switching from variant i to variant j. The probability of an antigenic switch per parasite division is fixed and is equal to σ (Turner and Barry 1989). This implies that the switch rates $\mathbf{S} = (s_{ij})_{N\times N}$ satisfy

$$\sum_j s_{ij} = \frac{r\sigma}{\ln(2)}. \quad (5)$$

Table 1: Model parameters and interpretation

Parameter	Interpretation (units)	Dimensional value	Reference/comment
r	Intrinsic growth rate of slender cells (h^{-1})	1×10^{-1}	Turner et al. 1995
d	Maximal killing efficiency of slender cells by the immune response (h^{-1})	5×10^{-1}	McLintock et al. 1993
δ	Maximal killing efficiency of stumpy cells by the immune response (h^{-1})	1×10^{-1}	McLintock et al. 1993
c	Rate of growth of specific immune response (h^{-1})	1×10^{2}	Lythgoe et al. 2007
K	Within-host carrying capacity for the total parasite population	$1 \times 10^{8}-1 \times 10^{12}$	Reuner et al. 1997; varied
C	Threshold variant population level leading to maximal growth of specific immune response	$1 \times 10^{8}-1 \times 10^{12}$	Lythgoe et al. 2007; varied
x	Sensitivity of immune responses to small parasite concentration	1–3	Lythgoe et al. 2007; varied
τ	Delay in the stimulation of specific immunity (hours)	100	Tyler et al. 2001; varied
δ_M	Stumpy cell mortality rate (h^{-1})	2.5×10^{-2}	Tyler et al. 2001; Savill and Seed 2004
σ	Switch probability per division	1×10^{-2}	Turner and Barry 1989
s_{ji}	Switch rate from j to i (h^{-1})	Varied	$\sum_j s_{ij} = \sigma r/\ln 2$[a]
N	Total number of variants	$O(10^3)$	Berriman et al. 2005
η	Number of variants in one block	1–100	Varied
B	Number of blocks in S	$B = N/\eta$	Varied

[a] See "Switch Matrix Procedure."

Then, to compute first-arrival times, we consider $P_i(t)$, the probability that variant i has not yet emerged by time t. The dynamics of $P_i(t)$ are governed by

$$\frac{dP_i}{dt} = -P_i \sum_{j \neq i} s_{ji} v_j, \tag{6}$$

collecting the switching contributions from all other variants into variant i. Note that $P_i(0) = 1$ for all variants i except the inoculating variant. To calculate t_i, a random number is drawn from the uniform distribution $[0, 1]$. When P_i reaches this value, v_i jumps to 1, and from this point onward v_i, m_i, and a_i, so far inactive, begin the deterministic dynamics given by equations (1)–(3). Thus, the switching process matters only as a mechanism for generating previously absent antigenic variants, and its contribution to parasite growth is negligible.

Motivated by the subfamily structure of the trypanosome antigen gene archive (Morrison et al. 2005; Marcello and Barry 2007*a*), we assume the switch matrix **S** is characterized by a block structure (see **S** in fig. 1*B*), where within-block switching (diagonal blocks) happens at a faster rate than between-block switching (off-diagonal blocks). In the limit of very small between-block switch rates, variants of different blocks grow independently. Finally, the full model is given by equations (2)–(6), with parameters listed in table 1. The system is solved numerically in Matlab, using solver dde23. The initial conditions are $v_1 = V_0$, $v_{i\neq 1}(0) = 0$, $m_i(0) = 0$, and $a_i(t) = 0$, for $t \in [-\tau, 0]$ and for all i. We use the Events option of dde23 to pause and resume integration at the first-arrival times of new variants.

Model Behavior

A typical infection profile obtained from the model captures the main features of real trypanosome infections: (1) Within-host dynamics are characterized by oscillating total parasite load (fig. 2), where each peak is composed of different antigenic variants (Barry and McCulloch 2001). Although infection may be initiated by a single variant, stochastic antigenic variation quickly gives rise to new variants, thus prolonging the infection. (2) Consistent with empirical observations (Miller and Turner 1981; Robinson et al. 1999), an infection peak can be composed of one or more variants, depending on the switch matrix. (3) Numerical simulations confirm that variant first-arrival times highly correlate with variant mean activation rates from the switch matrix. The higher the variant activation rate, the earlier a particular variant appears during infection, as reported also by Marcello and Barry (2007*a*). Early variants are also associated with a smaller variability in first-arrival times across stochastic simulations, consistent with empirical findings (Morrison et al. 2005; Marcello and Barry 2007*a*). Since the switch rates within a block are larger than between blocks, all the variants in a block emerge at similar times. (4) When the switch matrix follows the nonhierarchical mode (fig. 1*B*), consecutive par-

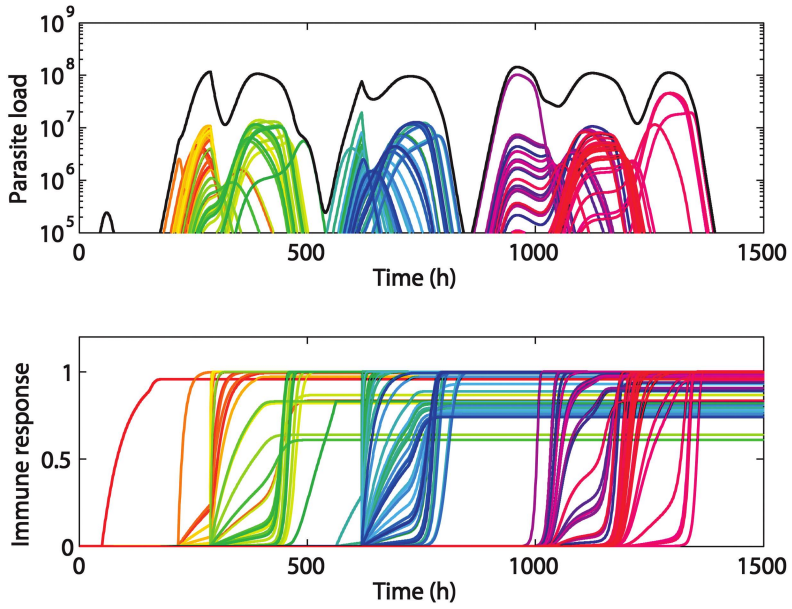

Figure 2: Example of full model dynamics with $N = 120$, $\eta = 12$, $x = 2$, $K = 10^8$, $C = 10^7$, and other parameters as in table 1. The black line shows the total parasite load $V + M$, and the colored lines indicate individual variants $v_i + m_i$. The switch matrix used follows the nonhierarchical mode in figure 1*B*.

asite peaks have generally equal spacing, and the order of variant appearance is determined by the position of the inoculating variant in the matrix and the sequence of its neighboring blocks; if the switch matrix is hierarchical, consecutive parasite peaks occur at increasingly greater temporal distances, and the order of variant appearance is independent of the inoculating variant.

The behavior of the model is complex, resulting from the interplay of many parameters. The results we present here are robust even when dropping the perfect symmetry across variants in the model, that is, allowing variability within the same order of magnitude, in growth rates, rates of differentiation, immunogenicity, and delay in immune stimulation. These changes do not change the model's qualitative or, to a large extent, quantitative behavior. To understand the mechanisms behind trypanosome within-host dynamics, it is helpful to begin by first examining what governs a single infection peak and then what drives the full infection profile within a host.

Single-Block Dynamics

Block size $\eta = 1$. The dynamics of a single variant can be broken down into three phases: I, growth; II, nongrowth; and III, the decline phase, as illustrated in figure 3. These three phases also appear in the full infection profile. In phase I, the variant grows at an exponential rate, mediated by fast proliferation of slender cells v_i. As the total parasite population increases, cells begin to transform to the stumpy form m_i in a density-dependent manner; thus, the effective growth rate of the parasite population is reduced. However, specific antibody responses continue to increase as $v_i + m_i > 0$. Once $V + M \approx K$, we enter phase II, where $V + M \approx K$ until $a_i = r/d$ for any i, signaling the end of phase II. Asymptotic analysis of the model reveals that a necessary requirement for the stability of the infection clearance equilibrium is $a_i > r/d$. If $a_i = r/d$ before $V + M \approx K$, then phase II is not initiated. In fact, as soon as a_i surpasses this threshold, phase III of the dynamics begins, leading to the decline of each variant.

Notice that in general phases I and III always happen because there is no prior immunity against any variant, permitting growth, and the build-up of the immune response due to antigen stimulation will lead to eventual decline. Phase II is more complex, and it is key in determining the dynamics. Depending on whether phase II is long or short, a variant may take a longer or shorter time to be cleared. The duration of phase II is inextricably linked to the strength of specific immunity. The weaker specific immunity is during phase I (e.g., large τ, x, C), the more the parasite can grow and the longer it takes for a_i to reach r/d, hence, the longer phase II. In contrast, the stronger specific immunity, the less the parasite can grow and the faster it is cleared, shortening phase II or removing it altogether.

Block size $\eta > 1$. The variants in an infection peak usually

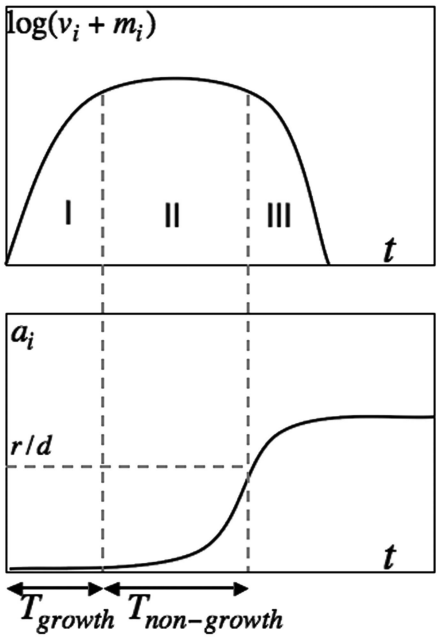

Figure 3: Schematic of individual variant infection dynamics illustrating the specific immune response (*bottom*) and variant growth (*top*) with three phases: I = growth, II = nongrowth, and III = decline. The total duration of these three phases defines a block wave.

correspond to variants of the same block in the switch matrix S, and we notice that their first-arrival times are clustered (see fig. 2). Thus, to study a single infection peak, we can study a single block of variants, by assuming the variants of a block emerge around the same time: $t_i \approx t_j$, for each variant i and j within a block. We assume there is an initial parasite load V_0, which is divided equally among the η variants, and there is no prior host exposure to any of the antigens.

In the same way that each variant dynamics is composed of three phases, the dynamics of a block is composed of the growth, nongrowth, and decline phase. But now the number of variants growing together matters. Ultimately, specific immune stimulation depends on the availability of antigen, hence on the magnitude of $v_i + m_i$. This goes down as the number of variants η sharing the carrying capacity K within the host increases. Model simulations show that as η increases, the duration of phase II of the dynamics tends to infinity, because the numbers of any individual variant are low, $\sim K/\eta$, resulting in weak immune stimulation, and so a_i struggles to reach r/d (see fig. 4). It is then natural to ask, what is the critical η dividing these distinct dynamical regimes, of rapid block clearance and long block persistence?

The Block Size Threshold η_{crit}

To distinguish between fast and slow infection clearance, we analyze the duration of phase II, $T_{\text{nongrowth}}$, via simple quasi-steady state arguments (see "Critical Block Size Threshold"). We define $T_{\text{nongrowth}} < 2\tau$ as fast clearance and $T_{\text{nongrowth}} > 2\tau$ as slow clearance. We find that $T_{\text{nongrowth}} > 2\tau$ when the number of variants in one block exceeds

$$\eta_{\text{crit}} = \frac{K}{C}\left[\frac{-\ln(1 - r/d)}{c\tau}\right]^{-1/x}. \tag{7}$$

This means that when the block size is relatively small, that is, $\eta < \eta_{\text{crit}}$, specific immunity rapidly clears all variants of that block, and hence, phase II is short; whereas for $\eta \geq \eta_{\text{crit}}$, differentiation regulates the parasite load, and so phase II is very long. When phase II is long, individual variants of a block are limited to low levels, insufficient to optimally stimulate specific immune responses. This allows them to persist at low densities, until sufficient host immunity is mounted. Similar thresholds have been found previously in antigenic variation models (Nowak et al. 1990; Sasaki 1994). In contrast to those results, our result refers to a quasi–steady state and applies only to variants whose first-arrival times are the same. For variants arising in the host at different times, the same threshold does not hold. Sufficient decoupling may allow them to grow independently and stimulate specific immunity.

The threshold η_{crit} depends linearly on K/C, the ratio between the within-host carrying capacity and the immune response threshold, expressing the competition between density-dependent differentiation and host immunity (fig. 4). When K/C increases, η_{crit} increases, meaning that the immune stimulation to individual variants is stronger; hence, there is sufficient specific control that can clear larger blocks of variants. When C/K increases, η_{crit} is reduced, implying dominance of general control; hence, even smaller blocks can easily persist without clearance.

The significance of this threshold for within-host dynamics points toward the interaction between specific and general control. This interplay is critical in many pathogen infections besides trypanosomes. In trypanosomes, in particular, properties of their antigenic archive, such as the size of an antigenic block, appear crucial and may tip the balance toward one mechanism of parasite control or the other. We notice how the ultimate duration of phases I + II + III, defining a block wave, depends on the block size η. This affects also the total parasite load, $\int(V + M)dt$, contained in a block wave (fig. 4), which may have implications for transmission.

In general, the η_{crit} phenomenon holds whenever the differentiation rate $f(V + M)$ increases in a nonsaturating manner with $V + M$, even when the specific immune re-

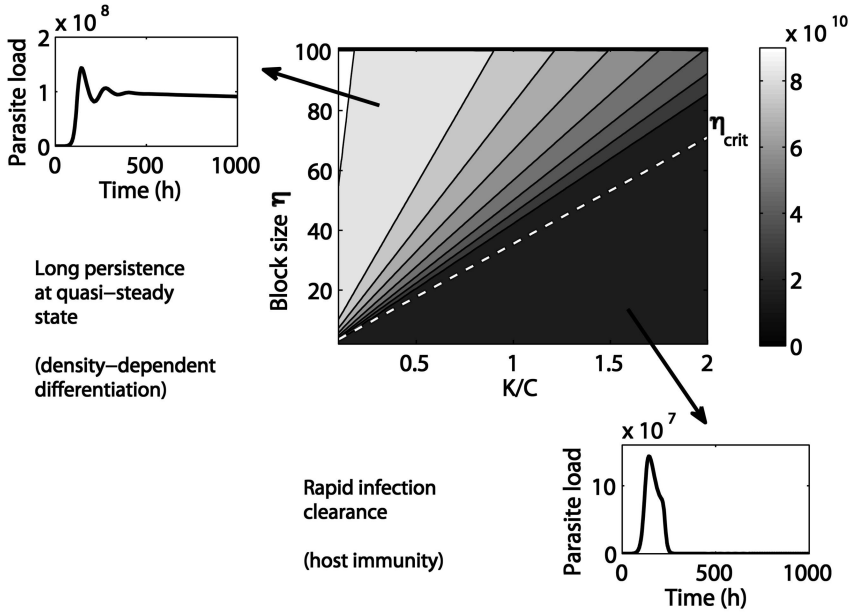

Figure 4: Contour plot of total parasite load $\int_0^{1,000} V(t) + M(t)dt$ as a function of block size η and K/C. The analytical approximation to η_{crit} (*dashed line*) is in good agreement with the model's numerical simulation results. Parameter combinations where $\eta < \eta_{crit}$ (*dark gray regions*) lead to rapid variant clearance and generally lower peak parasite load. Parameter combinations where $\eta > \eta_{crit}$ (*light gray regions*) lead to extended persistence of variants and peak parasite load close to carrying capacity. The insets show rapid clearance ($\eta = 20$, $C = 2K/3$) and long persistence ($\eta = 80$, $C = 2K$). Parameters as in table 1, and $K = 10^8$, $x = 3$.

sponse is saturating with respect to $v_i + m_i$ (e.g., Holling type II). In contrast, if $f(V + M)$ saturates with increasing total parasite load, η_{crit} does not always hold, in particular when host immunity is nonsaturating with respect to $v_i + m_i$. Next we explore the sensitivity of other infection characteristics such as the peak parasite number, variant subpeaks, and slender/stumpy ratio to η.

Why Does the Block Size (η) Matter?

Our model captures a continuum of dynamic scenarios from the limit of K, very large relative to C, to the limit of C, very large relative to K. In the former case, specific host immunity dominates, and all variants of the block are quickly controlled by the action of specific antibodies and phase II is short. In the latter case, differentiation dominates, determining the peak at carrying capacity and extending phase II. Let us consider the first limit: K tends to infinity. So, parasite numbers are controlled only by specific immunity, and the dynamics of each variant are decoupled from each other. Assuming for a moment the delay $\tau = 0$ and $x = 1$, we study the case where the sensitivity of the immune response to parasite numbers is at its strongest. As a consequence, the total peak V_{max} increases with the number of variants present in the block, while the size of individual variant peaks $(v_i)_{max}$ and block wave duration remain unaffected. In this case, only slender cells are present, because density dependence mediating stumpy cell production is absent.

Now consider the second limit: C tends to infinity. We now have only general control through density-dependent differentiation. This implies that the variants in the block are completely coupled in their dynamics. In this case, $(V + M)_{max}$ is determined by the within-host carrying capacity K, independent of block size. Conversely, individual variant peaks, $(v_i + m_i)_{max}$ decrease linearly with η, because variants now share the carrying capacity. The ratio of slender-to-stumpy numbers initially favors the slender forms during phase I, and the ratio gradually tends toward δ_M/r during phase II. Because $\delta_M < r$, differentiation-only control favors prevalence of the stumpy transmission forms of the parasite.

Finally, the case of moderate C and K lies in between the two scenarios. By varying η, the dynamics smoothly approaches one extreme or the other and the infection characteristics show a different dependence on block size (fig. 5). At the start of the infection $a_i(0) = 0$, the dynamics of stumpy cells initially depends entirely on that of slender cells, with $dm_i/dt = r\eta v_i^2/K$. When $r\eta/K$ is sufficiently small, that is, $r\eta/K \ll c/C$, then the number of

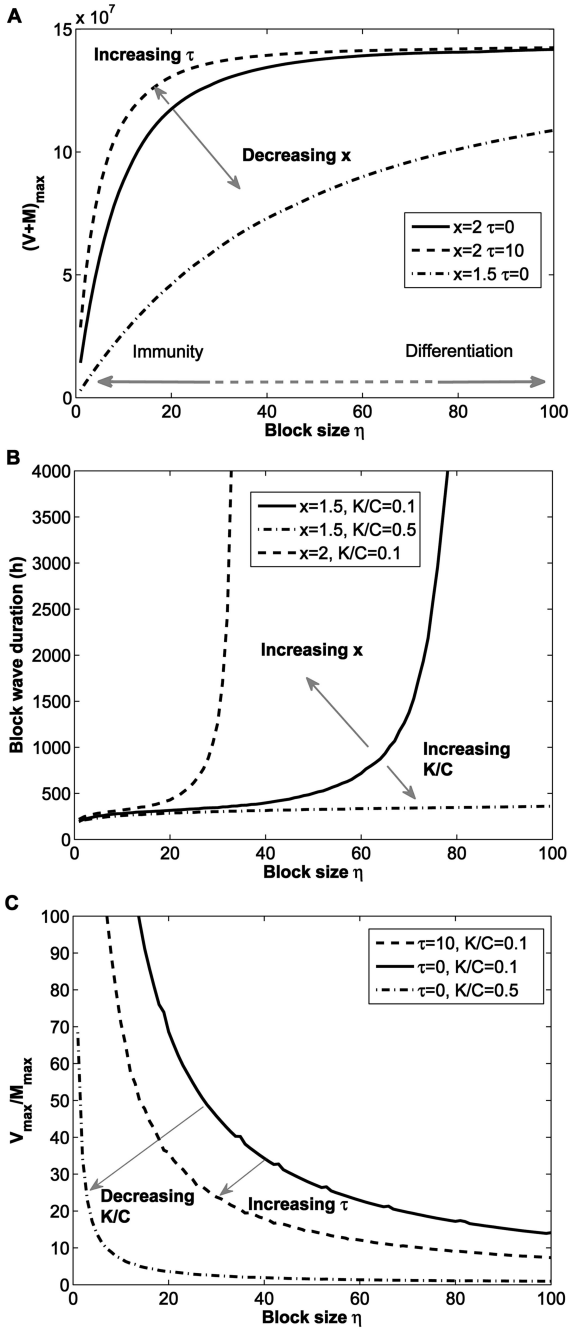

Figure 5: Infection characteristics as a function of η. *A*, Peak parasite load increases with η when host immunity dominates in parasite control. *B*, Block wave duration increases with η when differentiation is dominant for large block sizes. *C*, Slender-to-stumpy ratio decreases with η toward the value r/δ_M mediated by differentiation dominance. The dashed and dash-dotted lines illustrate that the effects of differentiation are accelerated by larger immune delay τ and small K/C, whereas immunity dominance is favored by small x and small τ. Parameter values: $K = 10^8$, $C = 10^9$ (*A*); $\tau = 0$, $K = 10^8$ (*B*); $x = 1.7$, $K = 10^8$ (*C*). All other parameters are as in table 1. Duration is calculated as the time it takes for $V + M$ to fall below its initial value $V_0 = 10^3$.

stumpy cells is small because parasite differentiation happens more slowly than immune action. This implies that slender–immune system interaction governs the parasite population dynamics, giving predominance of slender forms $(v_i)_{max} \gg (m_i)_{max}$, and hence, $V_{max} \gg M_{max}$. Because of the weak coupling between variants, V_{max}, M_{max}, and $(V + M)_{max}$ all increase with the block size η, even though the absolute magnitude of parasite load and block wave duration is low. When $r\eta/K$ exceeds c/C, differentiation happens faster and this results in higher stumpy cell production. As η increases, the stumpy cells catch up with the slenders during infection and even reach a higher peak. Thus, the slender-to-stumpy ratio V_{max}/M_{max} decreases, with η tending toward the value determined by differentiation dominance (fig. 5*C*).

In general, the relative dominance of specific over general parasite control can be counterbalanced by opposite changes in parameters. Block wave duration, for example, increases as a function of η faster when x is large but more slowly instead when the ratio K/C is large (fig. 5*B*). When we also consider cases where $\tau > 0$ and $x \geq 1$, numerical simulations reveal that differentiation dominance occurs at even smaller block sizes than when $\tau = 0$ and $x = 1$ (fig. 5*A*). A large delay τ or large x favors the decoupling between current levels of parasite load and immune response. This decoupling generally results in the individual variant dynamics being controlled more strongly via density-dependent differentiation. In summary, in immunity-dominant scenarios, the peak parasite load increases with η, whereas in differentiation-dominant scenarios, block wave duration increases with η. These two quantities, together with stumpy-to-slender dominance, clearly have an important bearing on parasite transmission, resulting thus in a high selective pressure on the block size η.

Multiple-Block Dynamics $N = B\eta$

So far, we have focused only on a subset of the antigenic archive, namely, variants that emerge at the same time within the host, neglecting their switching. In the following, we analyze stochastic switching between blocks leading to the dynamics of the full model (fig. 2), where new variants arise at different times. In order to obtain infection dynamics exhibiting multiple peaks, the archive must be composed of many blocks (i.e., $B > 1$), each block in isolation must be relatively small (i.e., $\eta < \eta_{crit}$), and the overlap between consecutive block waves in an infection must also be small; that is, between-block switching must be small ($\varepsilon \ll 1$).

The Critical Variant Activation Rate

A unique feature of the stochastic model and observed in experiments is that some variants never arise during infection. To understand this phenomenon, we go back to the entries of the switch matrix **S**. We define the mean activation rate of a new variant i in the system approximately as

$$\bar{s}_i = \frac{1}{\eta} \sum_{j \in \text{current block}} s_{ji}, \tag{8}$$

under the assumption that the major contribution in switching comes from the block of variants currently growing in the host. Through $\bar{s}_i$, the variants of any new block can be ranked, from high activation rate ($\bar{s}_i$ large) to low activation rate variants ($\bar{s}_i$ small). Besides the higher-level organization of variants in units of blocks, there is thus another layer of hierarchy in terms of mean activation rates, which fine-tunes sequential variant appearance within a block. Notice from the construction of the switch matrix that these mean activation rates all belong to the same order of magnitude εq, where q is the within-block average switch rate and $\varepsilon \ll 1$.

Recall that $P_i(t)$ is the probability that variant i has not yet emerged in the host by time t. Substituting equation (8) into the original equation for P_i, we get the simpler equation

$$\frac{dP_i}{dt} = -P_i \bar{s}_i V, \tag{9}$$

where $V(t)$ is the slender-cell population from the current block of variants. Solving equation (9) gives

$$P_i(t) = \exp\left(-\bar{s}_i \int_0^t V(s)ds\right). \tag{10}$$

In order to better understand stochastic variant generation, we simplify the analysis (for details, see "The Critical Activation Rate s_{crit}" in the appendix) by assuming the same stochastic generation threshold for each variant, following the deterministic approximation approach used by Kepler and Perelson (1995). If a variant is never generated, this means that the probability $P_i(t)$ never reaches the required generation threshold. The explanation lies in the interaction between variant mean activation rate $\bar{s}_i$ and the total slender cell number within a block $\int_0^t V(s)ds$. Notice that when a block contains a few variants, the integral $\int_0^t V(s)ds$ is bounded, as all phases of the dynamics are short. This leads to a critical lower bound for $\bar{s}_i$ (see "The Critical Activation Rate s_{crit}" in the appendix):

$$s_{\text{crit}} = \frac{1}{2K\tau}, \tag{11}$$

such that for $\bar{s}_i < s_{\text{crit}}$ variant i of the new block will never be generated, and for $\bar{s}_i > s_{\text{crit}}$ variant i may be generated (fig. 6).

Unsurprisingly, s_{crit} is determined by K, the within-host carrying capacity, and τ, the delay in immune response activation. When K and τ are large, each block of variants grows to a higher level and persists longer within the host before being suppressed by the host's immune system, as discussed in "Single-Block Dynamics." The s_{crit} threshold, being low, in this case favors the parasite by allowing rare variants to play their part in the dynamics, thus prolonging infection. In general, any changes in parameter values that increase the total replicative potential, $\int_0^t V(s)ds$, of the current antigenic block lower s_{crit} and facilitate stochastic emergence for future blocks.

Interestingly, the carrying capacity K appears so far to have two very important roles in the full dynamics of the model: it controls the duration of phase II in each block wave, and at the same time it affects switching between consecutive blocks. Also, the immune response delay appears be involved in both critical thresholds, η_{crit} and s_{crit}, consistent with previous studies showing that delays in immune activation considerably affect the window of opportunity for the pathogen to exploit its host before being suppressed by the immune system (Fenton et al. 2006).

Effects of the Switch Matrix

There are three main properties of the antigenic archive reflected in the switch matrix of our model: the size of a single block η, the number of blocks B, and between-block switch rates determined by ε. We find that when single blocks get larger, infection duration increases, but if η is too large, infection persists indefinitely, independently of the number of blocks and their between-block connectivity.

If the number of blocks B increases, infection duration and the number of peaks increase almost linearly, without affecting the nature of the dynamics of each peak. We observe that archive modularity, that is, larger B, enhances the overall oscillatory behavior and the sharpness of individual peaks in infection, even when the total number of variants N is kept constant. We expect that a sharp parasite peak in a real infection may well indicate a small antigenic block and strong variant-specific immune control. If the shape of a peak appears rounder, this may

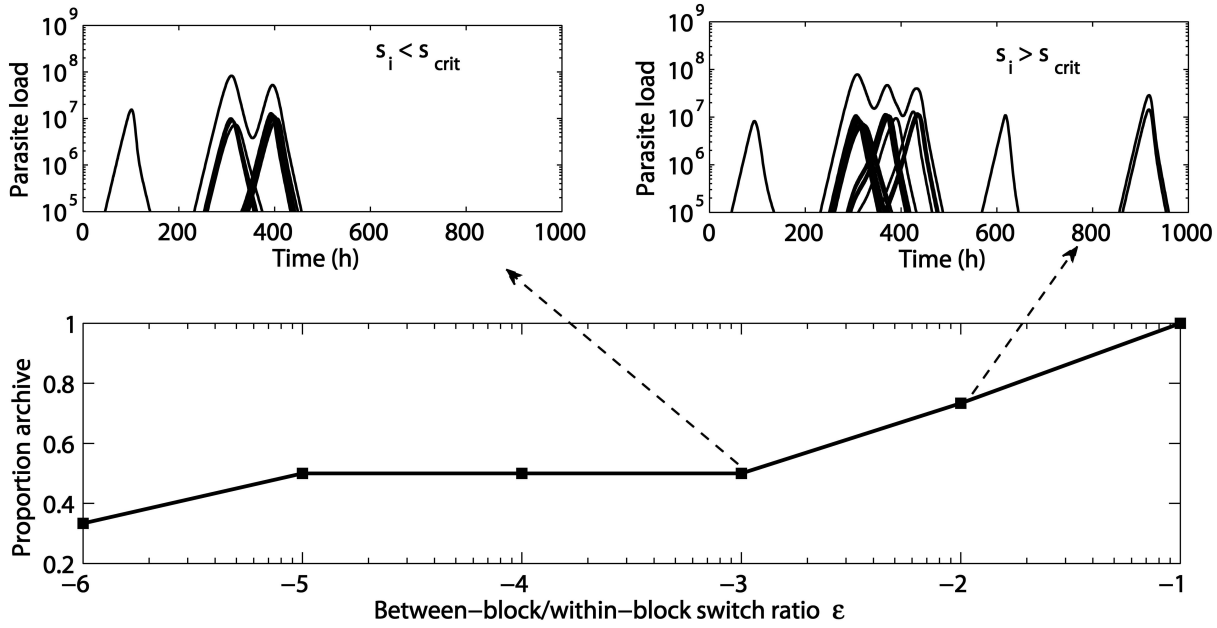

Figure 6: Role of ε in infection dynamics. When between-block switch rates are reduced, subsequent peaks occur farther and farther apart and a smaller proportion of the archive can be generated during infection, as more variants have mean activation rates below $s_{crit} = 1/(2K\tau) = 5 \times 10^{-8}$. The proportion of the archive refers to the number of variants expressed during infection over the total number of variants N. Parameter values: $K = C = 10^8$, $x = 3$, $\tau = 10$, $N = 30$, and $\eta = 5$. All other parameters are as in table 1. The switch matrix follows the hierarchical mode in figure 1*B*. A color version of this figure is available in the online edition of the *American Naturalist*.

suggest a larger number of variants contained therein and a weak immune control. An important feature of infection dynamics, then, the variability of peak densities, provides a further clue about dynamical mechanisms that may be responsible for parasite population cycles within the host. This property we find in infection dynamics is reminiscent of the critical interaction between top-down and bottom-up control, appearing widely in many other ecological contexts (see Turchin et al. 2000 for an example from lemming population cycles).

Finally, when between-block switch rates are lower, ε goes down, and the separation between block waves increases, giving longer infection duration overall. But there is a trade-off: if between-block switch rates are too low, variants of subsequent blocks may not be generated at all (fig. 6). This is related to the s_{crit} phenomenon discussed in the previous section. So if switching between blocks is low, the benefit from longer duration must offset the risk of stochastic parasite extinction.

Extensions of the Standard Model

The current model may be extended to capture a more realistic host immune response. Arguably, our formulation so far neglects decay in antibody responses, but this assumption is not an oversimplification for trypanosome infections, where immune memory plays a central role. Undoubtedly, when more data become available, a mechanistic description of antibody and memory B cell dynamics would be preferable to the phenomenological approach adopted here. However, we explore three other immune scenarios that might prove important: (1) the existence of prior immunity against some variants, (2) cross-reactivity between different variants, and (3) immunosuppression as a result of active infection in the host. Clearly, these extensions affect the dynamics mostly when host immunity dominates in controlling an infection.

Prior Immunity

The existence of prior immunity results in partially immune hosts either via prior exposure to infection or via vaccination, having provided some initial level of strain-specific immunity. We find that the size of a single block becomes especially important when there is prior immunity against some variants: the larger the block, the higher the chance for the parasite to establish an infection by switching sufficiently fast to a variant unseen before. Notice that phase I of the dynamics of any variant occurs only if the level of preexisting immunity against this var-

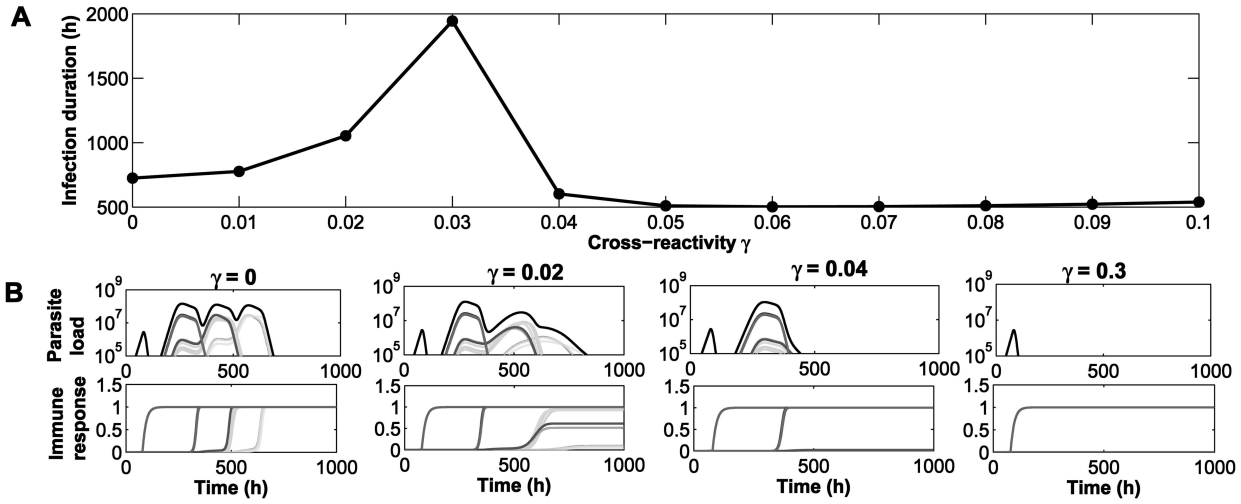

Figure 7: *A*, Infection duration as a function of between-block cross-reactivity γ. Intermediate values of cross-reactivity are good from the pathogen's perspective as they allow longer persistence and enhance transmission. *B*, As γ gets too large, not only is infection duration reduced but also stochastic emergence of new variants is made impossible, and only a small repertoire of variants is ever seen. Parameters as in table 1, with $N = 15$, $\eta = 5$, $K = C = 10^8$, $x = 2$, and S nonhierarchical as in figure 1*B*. Duration is calculated here as the time it takes for $V + M$ to fall below its initial value $V_0 = 10^3$. A color version of this figure is available in the online edition of the *American Naturalist*.

iant is low, more precisely if $a_i(0) < r/d$ and if $v_i(0) < K(1 - da_i(0)/r)$. If the size of the first block is too small, then there are only a few new variants available for expression, and the parasite risks immediate extinction in the partially immune host. This suggests another selective pressure on the size of single blocks in the antigenic archive of trypanosomes, namely, the requirement to seed an infection in partially immune host individuals.

Cross-Reactivity

There is evidence that trypanosome mosaic VSG variants emerging in the chronic stages of infection, with at least 75% sequence identity, exhibit high levels of cross-reactivity (Marcello and Barry 2007*b*). Variants within an antigenic block generally have a high sequence identity, whereas variants across blocks have a low sequence identity. In this context, by adding cross-reactivity into the model, we introduce positive coupling between specific immune responses, allowing existing immune responses against particular variants to partially clear other variants. The model is modified by replacing da_i and δa_i in equations (1) and (2) with $d\sum_{j=1}^{N} a_j\gamma_{ji}$ and $\delta\sum_{j=1}^{N} a_j\gamma_{ji}$, where γ_{ji} reflects the probability that antibodies raised against variant j can clear variant i. In other systems, including malaria, cross-reactivity has been proposed, at least on a theoretical level, to play a significant role on the order of variant expression (Recker et al. 2004). In trypanosome antigenic variation however, we find this is not the case.

We find that uniform cross-reactivity within a block acts as a general background immunity increasing the net clearance rate of each variant of that block. When the block size is large, this results in a lower peak parasite load, the opposite of what was seen in the immunity-dominant scenarios of "Why Does the Block Size (η) Matter?" However, when differentiation dominates in parasite control, cross-reactivity has no effect on the dynamics, as the growth inhibition of the parasite due to differentiation is generally much stronger and more significant than the growth inhibition due to cross-reactivity. Thus, variant peaks still decrease with η and the block wave duration increases with η, but with cross-reactivity, their sensitivity to η is higher.

Cross-reactivity between subsequent archive blocks adds into the model another factor of relatedness between parasite variants besides the switch matrix. Unlike the switch matrix that determines how fast the parasite moves in antigenic space, cross-reactivity marks how advantageous that movement really is.

Paradoxically, for intermediate values of uniform cross-reactivity between blocks, the parasite is able to prolong infection (see fig. 7), because persistent immunity raised against the early variants is sufficient to suppress later variants causing their specific antibody responses not to saturate quickly to maximum. This leads to lower levels of future parasite peaks within the host, as more variants emerge but are spread over a longer time scale, an effect previously shown also for *Plasmodium* (Recker and Gupta 2006).

For higher between-block cross-reactivity, however, unsurprisingly, clearance of future variants happens more rapidly, decreasing both the parasite load and infection duration. Furthermore, depending on the immune response sensitivity x, the level of cross-reactivity between consecutive antigenic blocks may play a role in determining the relative critical threshold for the new block size as a function of the size of the previous block. We find that in the presence of between-block cross-reactivity, there are cases when later antigenic blocks can persist more easily (η_{crit} smaller) if earlier antigenic blocks are large. This analysis suggests that immune cross-reactivity across trypanosome variants may be important in within-host infection progression, affecting not only the infection peak but also its overall duration, with potential implications for host health and infection transmission.

Immunosuppression

It has been shown that the host's capacity to control an infection may be limited: in inbred mice, the supply of naive B cells can decrease dramatically during a trypanosome infection, with the consequent decrease in the rate of production of specific antibodies (Radwanska et al. 2008). While the exact nature of immunosuppression may be determined by a series of different factors, we considered only the number of antigenic variants as a factor, which represents the most conservative case.

When immunosuppression results only from η variants within a block, equation (3) is replaced with

$$\frac{da_i}{dt} = \frac{c}{A(\eta)}\left[\frac{v_i(t-\tau) + m_i(t-\tau)}{C}\right]^x (1 - a_i), \qquad (12)$$

where $A(\eta) = \phi e^{\alpha\eta}/(\phi + e^{\alpha\eta} - 1)$. We find that in the presence of immunosuppression, increases in the block size η produce even higher increases in the peak total parasite load than previously shown. However, as differentiation becomes stronger with increasing η, effects from within-block immunosuppression become weaker, and the density-dependent effects from differentiation, which lower variant peaks, become dominant. So in general, for moderate immunosuppression, the qualitative behavior of the system is very similar to the inexhaustible immune response case analyzed throughout "Single-Block Dynamics."

However, when immunosuppression acts as a function of the cumulative number of variants generated over the whole infection, the effects can be more dramatic. Equation (3) is now

$$\frac{da_i}{dt} = \frac{c}{A(N_t)}\left[\frac{v_i(t-\tau) + m_i(t-\tau)}{C}\right]^x (1 - a_i), \qquad (13)$$

where N_t refers to the total number of variants generated up to time t. Simulations show that depending on the maximum level of immunosuppression ϕ, the growth rate of specific immune responses against later variants can be gradually reduced to very low levels that allow them to persist and possibly overwhelm the host.

Discussion

Although a large number of studies have addressed trypanosome within-host infections, focusing on isolated aspects of the dynamics like variant order (Seed 1978; Kosinski 1980; Agur et al. 1989; Turner and Barry 1989), the interaction of specific and cross-reactive host immunity, (Antia et al. 1996), the connectivity pathways between variants (Frank 1999; Lythgoe et al. 2007), and parasite density–dependent differentiation into the stumpy parasite form (Tyler et al. 2001; Savill and Seed 2004), none of the models therein have analyzed all those aspects together in one context. The current model binds all these elements in a common framework, offering deeper insight into trypanosome dynamics and closer integration of these dynamics with switching mechanics revealed by the increasing availability of parasite genetic data.

The model illustrates how the structure of the parasite antigenic archive dictates critical thresholds at the within-host level, which have important implications for infection. The balance between specific immunity and parasite differentiation, while determining many features of chronic infection, such as peak parasite load, duration, and slender/stumpy ratio, emerged to be very sensitive to the size of one antigenic block, η. Variance in the size of different blocks in the switch matrix can make this balance dynamic over the course of an infection, giving rise to variability in infection profiles. Another finding of the model is that demographic stochasticity, as shown also by Sasaki and Haraguchi (2000), can matter in within-host antigenic variation dynamics, in our case especially, since the switch rates between variants range over several orders of magnitude. The effects of stochastic variant emergence are particularly important early, when the parasite infects partially immune hosts, and generally in the chronic phase, where the maintenance of infection depends on rapid jumps between antigenic blocks. The minimum switch rate, s_{crit}, required for stochastic generation of a new variant is an emergent property of the model and is not dependent on the details of the switch matrix. In particular, when a hierarchical switch matrix is assumed (see fig. 1*B*), the critical switch rate requirement is even stronger.

Two different chronic infection scenarios arise from the model. A stationary chronic infection, where phase II lasts indefinitely, requires a single block to be large enough to allow differentiation to dominate parasite control within the host. In this case, the same variants persist throughout the infection, limited only by the carrying capacity. An oscillatory infection with multiple peaks (characteristic of typansome infection), requires small single blocks, so that immune-mediated clearance of each block is possible, and sufficiently high between-block switch rates to enable exploration of other antigen blocks. The latter scenario is characterized by sequential emergence of new variants. These two requirements correspond to the two critical thresholds derived in this article, η_{crit} and s_{crit}. Essentially, the parasite faces a trade-off for maximal use of its archive. Jumping to consecutive blocks should occur neither too fast, to avoid overwhelming the host, nor too slowly, to avoid premature infection clearance.

For a fixed archive instead, these two chronic scenarios (stationary and oscillatory) are attained for different levels of host immune competence. We expect that in immune-compromised hosts, stationary infection persistence is established more easily, whereas in immune-competent hosts, multiple-peak chronicity is established more easily. This model prediction is confirmed by some existing empirical studies (Hajduk and Vickerman 1981) but can be tested further experimentally. The relative differences between these two scenarios link also to the general differences between acute and chronic infection (Alizon and van Baalen 2008) and may have an important evolutionary significance for the parasite.

How Genomic Data Can Inform the Model

The precise values of antigenic switch rates, lying at the interface between parasite genetics and within-host dynamics, may be very difficult to extract empirically. In a top-down approach, they would require a longitudinal study of several parallel infections and multiple screenings for variant identification at each peak. This way, an antigenic network could be inferred statistically from co-occurrences of variants. A few studies over the first 3–5 weeks of infection do show that individual variants are predictable in time of appearance (Timmers et al. 1987; Robinson et al. 1999; Marcello and Barry 2007*a*), but more high-throughput approaches could be applied over longer infection periods. Our model construct referring to the block size η would correspond then to the size of clusters in this network. In a bottom-up approach, relative switch rates might be inferred from sequence analysis of VSG gene flanks, as was achieved by Barbour et al. (2006), who showed that gene flank characteristics dictate fine timing of expression of variants in the bacterium *Borrelia hermsii*.

If the switch rates between trypanosome VSG variants can be mechanistically derived from genetic processes in the antigenic archive, and if the rates of these genetic processes are measured, then parameters of the switch matrix such as η, N, and ε can be properly quantified, and moreover, the global structure of the switch matrix, whether hierarchical or nonhierarchical, can be elucidated. Clearly, a combination of bottom-up and top-down approaches provides an ideal framework, where the model can meet experiments.

Future Work and Perspectives

Whether a stationary or an oscillatory chronic infection confers a higher fitness to the parasite remains unclear. An oscillatory parasite load may be of selective advantage over a stationary one, because its cumulative negative effect over time on host survival might be smaller, thereby extending the transmission time window for the parasite. Alternatively, the two strategies may endow the parasite with equal fitness, arising in trypanosome strains adopting one archive strategy or the other. If these different strains cannot be found in the field, this might indicate that certain archive configurations are easier to attain genetically.

Next comes the question of how the critical thresholds at the level of a single host affect parasite fitness at the population level. We can now begin to ask, at which antigenic block size do the virulence effects from long parasite persistence start to outweigh the transmission benefits? How does this depend on the balance between parasite differentiation and host immunity? The model suggests that the continuum of differentiation-immunity scenarios may favor different antigenic block sizes, in order to maximize parasite load within the host. However, because trypanosomes are vector-borne parasites, after a given threshold, an increase in the number of variants under one peak (η) and in the total parasitemia, may only increase virulence of the infection. In this sense, we would expect very virulent strains, for example, strains with too-large blocks in their VSG repertoire to be strongly counterselected.

Although we have not embedded our within-host model into an epidemiological context, some critical links with transmission and virulence already can be seen to emerge through parameters such as the within-host carrying capacity K. Related to the rate of parasite differentiation, K plays a critical role as a ceiling for parasite population growth, affecting ultimately the replication and transmission potential of the parasite. Clearly, using the model to address infection across different host species would involve some perturbation of K. Presumably, the size of the host may influence K, serving as an ecological upper bound, and some experimental data supporting this idea

already exist (Barry 1986). However, more research is needed to properly connect K to trypanosome infection and antigenic variation. Possible avenues for elucidating K from experiments, just to mention a few, could be the empirical exploration of trypanosome quorum-sensing mechanisms, a better understanding of the kinetics of the stumpy induction factor triggering differentiation (Vassella et al. 1997), and the identification of host mechanisms that might be involved therein.

From the fact that the critical between-block switch rate depends on K, it seems plausible that parasite genetic processes, responsible for the VSG archive subfamily structure, must ultimately evolve toward some K-dependent optimum, ensuring sufficient separation between blocks but also a minimum degree of connectivity. Any host factor that reduces the parasite replication potential must be counterbalanced by increases in between-block switch rates (e.g., genetic identity between variant subfamilies) to ensure stochastic generation of new blocks. Again one can ask, but how large are the parasite transmission benefits from expressing a higher number of blocks within a host, compared to virulence costs? How does this depend on the particular type of host and its ecology? Further research in this direction, linking selection pressure at the within-host and epidemiological levels with the genetic processes operating on the parasite antigenic archive, could have important implications for our understanding of trypanosome evolutionary dynamics.

Acknowledgments

We would like to thank L. Marcello and L. Morrison for helpful discussion and the Wellcome Trust for funding. The work has been supported by a Kelvin-Smith PhD scholarship from the University of Glasgow. We also thank the anonymous reviewers for helpful comments on an earlier version of this manuscript.

APPENDIX

Mathematical Details

Switch Matrix Procedure

Begin with input parameters η, N, ε, and σ. The switch matrix $\mathbf{S}$ has N variants, distributed in blocks, each consisting of η variants. Blocks lie on the diagonal of the matrix. The off-diagonal blocks contain between-block switch rates. The nonhierarchical switch matrix is constructed as follows: (1) For each block, both on and off the diagonal, we generate $\eta \times \eta$ random uniform numbers in $[0, 1]$. (2) Then we normalize them so that each row sums up to 1. We compute the within-block average switch rate for blocks on the diagonal: $q = r\sigma(\varepsilon - 1)/[\ln(2)(\varepsilon^{N/\eta} - 1)]$. (3) We then apply the magnitude structure according to figure 1*B*. The ε^n indicates that the between-block switch rate is ε^n times the average within-block switch rate q. (4) Finally, $\mathbf{S}$ is normalized globally so that each row sums up to $r\sigma/\ln(2)$.

Critical Block Size Threshold

Assuming that specific immune responses initially change on a slower timescale than slender and stumpy cells, the effect of immunity-mediated clearance during the growth phase (phase I) can be neglected. Let T_{growth} denote the time it takes for the parasite population to reach the nontrivial quasi–steady state given by solving equations (1) and (2) with $a_i = 0$. As a result of the symmetry between variants, $v_i + m_i = K/\eta$ at $t = T_{\text{growth}}$. Based on the quasi–steady state assumption for the parasite population, and as a consequence of the delay τ in the stimulation of immune responses, a_i starts to change at time $t = T_{\text{growth}} + \tau$, obeying the following equation:

$$da_i/dt \approx c(1 - a_i)(K/\eta C)^x,$$

which implies

$$0 < a_i(t) \leq 1 - \exp[-ct(K/\eta C)^x],$$

for $t \geq T_{\text{growth}} + \tau$. This is the maximal rate of change for a_i; thus, the time it would take for a_i to reach the required r/d threshold for the initiation of infection clearance can be approximated by

$$a_i(T_{r/d}) = 1 - \exp[-cT_{r/d}(K/\eta C)^x] = r/d,$$

giving

$$T_{r/d} \approx -(K/\eta C)^{-x} \ln(1 - r/d)/c.$$

If $T_{\text{nongrowth}} \approx \tau + T_{r/d} \leq 2\tau$, the duration of phase II is relatively short, followed by fast decline in phase III. If $\tau + T_{r/d} > 2\tau$, the parasite numbers persist for a long time in the nongrowth phase. Assuming all other parameters are fixed, the value of η for which $T_{r/d} = \tau$ yields the critical number of variants η_{crit} dividing the two regimes of fast clearance and long persistence. Simple algebra reveals that

$$\eta_{\text{crit}} = K/C[-\ln(1 - r/d)/c\tau]^{-1/x},$$

such that for $\eta < \eta_{\text{crit}}$ specific immunity rapidly clears all variants of that block, whereas for $\eta \geq \eta_{\text{crit}}$ differentiation is the main controlling force.

The Critical Activation Rate s_{crit}

Adopting the deterministic threshold approximation of Kepler and Perelson (1995), we assume the same generation threshold $1/e$ for all new variants. Stochastic arrival times t_i are then replaced by discrete arrival times T_i. When $P_i(t)$ crosses the given threshold, $T_i = t$ and variant i is generated. The probability that variant i has not yet been generated by time t is rewritten as $P_i(t) = \exp(-\bar{s}_i \int_0^t V(s)ds)$ (see eq. [8]). Assuming that $\eta < \eta_{crit}$ and so $V = \eta v$, and thus $V \to 0$ as $t \to \infty$ for the current block, we proceed by bounding the integral $\int_0^t V(s)ds$ from above. Because $V(t) \geq 0$, for all t, we have $\int_0^t V(s)ds < \int_0^\infty V(s)ds$. It is easy to see that $V_{max} < V_{max} + M < K$. Now, denote by τ_K the time it takes for the slender population V to reach K growing exponentially from an initial population V_0. Recall from the previous section that $T_{nongrowth} \leq 2\tau$. We can now construct a piecewise upper bound for dV/dt using standard Heaviside functions $H(z)$, corresponding to each phase of the dynamics illustrated in figure 3, as follows:

$$\begin{aligned}\frac{dV}{dt} &= r\left(1 - \frac{V+M}{K}\right)V - daV < H(\tau_K - t)rV \\ &\quad + H(t - \tau_K - 2\tau)\left(rV - r\frac{V^2}{K} - daV\right) \\ &< H(\tau_K - t)rV - H(t - \tau_K - 2\tau)r\frac{V^2}{K} \\ &:= \frac{dV_u}{dt}.\end{aligned}$$

We have used the fact that host immunity ensures $a > r/d$ throughout phase III, that is, for time $t \geq \tau_K + 2\tau$, and also the fact that in the decline phase, stochastic extinction of the parasite population occurs if V falls below some critical value, $V_{ext} \ll 1$. This happens at time $T_{ext} = 1/r(K/V_{ext} - 1)$. Thus,

$$\begin{aligned}\int_0^\infty V_u(s)ds &= \int_0^{T_{ext}} V_u(s)ds \\ &= K\left[\frac{1}{r} + 2\tau + \frac{1}{r}\log\left(\frac{K}{V_{ext}}\right)\right].\end{aligned}$$

Notice the dependence of the last expression on K, r, τ, and V_{ext}, among which the major contribution is played by the term $2\tau K$. In fact, for suitably small V_{ext}, the contribution of both terms $1/r$ and $1/r\log(K/V_{ext})$ inside the bracket is $o(\tau)$. This way, $\int_0^\infty V(s)ds < \int_0^\infty V_u(s)ds \approx 2K\tau$. Thus, we define the critical activation rate as $s_{crit} = 1/2K\tau$, such that if $\bar{s}_i < s_{crit}$, we have

$$\begin{aligned}P_i(t) &> \exp\left(-\bar{s}_i \int_0^\infty V(s)ds\right) \\ &> \exp\left(-s_{crit} \int_0^\infty V(s)ds\right) > \exp(-1) \\ &= 1/e, \forall t,\end{aligned}$$

which means variant i will never be generated.

Literature Cited

Agur, Z., D. Abiri, and L. H. Van der Ploeg. 1989. Ordered appearance of antigenic variants of African trypanosomes explained in a mathematical model based on a stochastic switch process and immune selection against putative switch intermediates. Proceedings of the National Academy of Sciences of the USA 86:9626–9630.

Alizon, S., and M. van Baalen. 2008. Acute or chronic? within-host models with immune dynamics, infection outcome, and parasite evolution. American Naturalist 172:E244–E256.

Antia, R., M. A. Nowak, and R. Anderson. 1996. Antigenic variation and the within-host dynamics of parasites. Proceedings of the National Academy of Sciences of the USA 93:985–989.

Balber, A. 1972. *Trypanosoma brucei*: fluxes of the morphological variants in intact and x-irradiated mice. Experimental Parasitology 31:307–319.

Barbour, A. G., Q. Dai, B. I. Restrepo, H. G. Stoenner, and S. A. Frank. 2006. Pathogen escape from host immunity by a genome program for antigenic variation. Proceedings of the National Academy of Sciences of the USA 103:18290–18295.

Barry, J. 1986. Antigenic variation during *Trypanosoma vivax* infections of different host species. Parasitology 92:51–65.

———. 1997. The relative significance of mechanisms of antigenic variation in African trypanosomes. Parasitology Today 13:212–218.

Barry, J., and R. McCulloch. 2001. Antigenic variation in trypanosomes: enhanced phenotypic variation in a eukaryotic parasite. Advances in Parasitology 49:1–70.

Berriman, M., E. Ghedin, C. Hertz-Fowler, G. Blandin, H. Renauld, D. Bartholomeu, N. Lennard, E. Caler, N. Hamlin, and B. Haas. 2005. The genome of the African trypanosome *Trypanosoma brucei*. Science 309:416–422.

Capbern, A., C. Giroud, T. Baltz, and P. Mattern. 1977. *Trypanosoma equiperdum*: étude des variations antigéniques au cours de la trypanosomose expérimentale du lapin. Experimental Parasitology 42:6–13.

Dean, S., R. Marchetti, K. Kirk, and R. Matthews. 2009. A surface transporter family conveys the trypanosome differentiation signal. Nature 459:213–217.

Fenton, A., J. Lello, and M. Bonsall. 2006. Pathogen responses to host immunity: the impact of time delays and memory on the evolution of virulence. Proceedings of the Royal Society B: Biological Sciences 273:2083–2090.

Frank, S. A. 1999. A model for sequential dominance in African trypanosome infections. Proceedings of the Royal Society B: Biological Sciences 266:1397–1401.

———. 2002. Immunology and evolution of infectious disease. Princeton University Press, Princeton, NJ.

Gray, A. 1965. Antigenic variation in a strain of *Trypanosoma brucei* transmitted by *Glossina morsitans* and *G. palpalis.* Journal of General Microbiology 41:195–214.

Hajduk, S., and K. Vickerman. 1981. Antigenic variation in cyclically transmitted *Trypanosoma brucei*: variable antigen type composition of the first parasitaemia in mice bitten by trypanosome-infected *Glossina morsitans.* Parasitology 83:609–621.

Kepler, T., and A. Perelson. 1995. Modeling and optimization of populations subject to time-dependent mutation. Proceedings of the National Academy of Sciences of the USA 92:8219–8223.

Kosinski, R. 1980. Antigenic variation in trypanosomes: a computer analysis of variant order. Parasitology 80:343–357.

Luckins, A. 1972. Effects of x-irradiation and cortisone treatment of albino rats on infections with *brucei*-complex trypanosomes. Transactions of the Royal Society of Tropical Medicine and Hygiene 66:130–139.

Lythgoe, K., L. J. Morrison, A. Read, and J. Barry. 2007. Parasite-intrinsic factors can explain ordered progression of trypanosome antigenic variation. Proceedings of the National Academy of Sciences of the USA 104:8095–8100.

Marcello, L., and J. Barry. 2007*a*. Analysis of the VSG gene silent archive in *Trypanosoma brucei* reveals that mosaic gene expression is prominent in antigenic variation and is favored by archive substructure. Genome Research 17:1344–1352.

———. 2007*b*. From silent genes to noisy populations—dialogue between the genotype and phenotypes of antigenic variation. Eukaryotic Microbiology 54:14–17.

McLintock, L., C. Turner, and K. Vickerman. 1993. Comparison of the effects of immune killing mechanisms on *Trypanosoma brucei* parasites of slender and stumpy morphology. Parasite Immunology 15:475–480.

Miller, E., and M. Turner. 1981. Analysis of antigenic types appearing in first relapse populations of clones of *Trypanosoma brucei.* Parasitology 82:63–80.

Morrison, L., P. Majiwa, A. Read, and J. Barry. 2005. Probabilistic order in antigenic variation of *Trypanosoma brucei.* International Journal for Parasitology 35:961–972.

Nowak, M., R. May, and R. Anderson. 1990. The evolutionary dynamics of HIV-1 quasispecies and the development of immunodeficiency disease. AIDS 4:1095–1103.

Radwanska, M., P. Guirnalda, C. De Trez, B. Ryffel, S. Black, and S. Magez. 2008. Trypanosomiasis-induced B cell apoptosis results in loss of protective anti-parasite antibody responses and abolishment of vaccine-induced memory responses. PLoS Pathogens 4: e1000078.

Recker, M., and S. Gupta. 2006. Conflicting immune responses can prolong length of infection in *Plasmodium falciparum* malaria. Bulletin of Mathematical Biology 68:821–835.

Recker, M., S. Nee, P. Bull, S. Kinyanjui, K. Marsh, C. Newbold, and S. Gupta. 2004. Transient cross-reactive immune responses can orchestrate antigenic variation in malaria. Nature 429:555–558.

Reuner, B., E. Vassella, B. Yutzy, and M. Boshart. 1997. Cell density triggers to stumpy differentiation of *Trypanosoma brucei* bloodstream forms in culture. Molecular and Biochemical Parasitology 90:269–280.

Robinson, N., N. Burman, and S. E. Melville, and J. Barry. 1999. Predominance of duplicative VSG gene conversion in antigenic variation in African trypanosomes. Molecular and Cellular Biology 19:5839–5846.

Sasaki, A. 1994. Evolution of antigen drift/switching: continuously evading pathogens. Journal of Theoretical Biology 168:291–308.

Sasaki, A., and Y. Haraguchi. 2000. Antigenic drift of viruses within a host: a finite site model with demographic stochasticity. Journal of Molecular Evolution 51:245–255.

Savill, N., and J. Seed. 2004. Mathematical and statistical analysis of the *Trypanosoma brucei* slender to stumpy transition. Parasitology 128:53–67.

Schmid-Hempel, P. 2008. Parasite immune evasion: a momentous molecular war. Trends in Ecology & Evolution 23:318–326.

Seed, J. 1978. Competition among serologically different clones of *Trypanosoma brucei gambiense* in vivo. Protozoology 25:526–529.

Thon, G., T. Baltz, C. Giroud, and H. Elsen. 1990. Trypanosome variable surface glycoproteins: composite genes and order of expression. Genes and Development 4:1374–1383.

Timmers, H., T. De Lange, J. Kooter, and P. Borst. 1987. Coincident multiple activations of the same surface antigen gene in *Trypanosoma brucei.* Journal of Molecular Biology 194:81–90.

Turchin, P., L. Oksanen, P. Ekerholm, T. Oksanen, and H. Henttonen. 2000. Are lemmings prey or predators? Nature 405:562–565.

Turner, M. 1999. Antigenic variation in *Trypanosoma brucei* infections: an holistic view. Journal of Cell Science 112:3187–3192.

Turner, M., and J. Barry. 1989. High frequency of antigenic variation in *Trypanosoma brucei rhodesiense* infections. Parasitology 99:67–75.

Turner, M., N. Aslam, and C. Dye. 1995. Replication, differentiation, growth and the virulence of *Trypanosoma brucei* infections. Parasitology 111:289–300.

Tyler, K., P. G. Higgs, K. Mathews, and K. Gull. 2001. Limitation of *Trypanosoma brucei parasitaemia* results from density-dependent parasite differentiation and parasite killing by the host immune response. Proceedings of the Royal Society B: Biological Sciences 268:2235–2243.

Vassella, E., B. Reuner, B. Yutzy, and M. Boshart. 1997. Differentiation of African trypanosomes is controlled by a density sensing mechanism which signals cell cycle arrest via the cAMP pathway. Journal of Cell Science 110:2661–2671.

Associate Editor: Yannis Michalakis
Editor: Ruth G. Shaw